IVYSPRING INTERNATIONAL PUBLISHER

Journal of Cancer

2024; 15(8): 2380-2390. doi: 10.7150/jca.92780

Research Paper

Erianin promotes apoptosis and inhibits Akt-mediated aerobic glycolysis of cancer cells

Shuangze Han[2#], Sijin Chen[3#], Jidong Wang[4#], Sheng Huang[5], Yeqing Xiao[6], Gaoyan Deng[1]✉

1. Department of Thoracic Surgery, Hunan Chest Hospital, Changsha 410013, Hunan, China.
2. Department of Ultrasound, Union Hospital, Tongji Medical College, Huazhong University of Science and Technology, Wuhan 430022, China.
3. Department of Urology, Hunan Provincial People's Hospital, The First Affiliated Hospital of Hunan Normal University, Changsha 410005, Hunan, China.
4. Department of Oral and Maxillofacial Surgery, Changde Hospital, Xiangya School of Medicine, Central South University (The first people's hospital of Changde city), Changde 415000, Hunan, China.
5. Department of General, Hunan Chest Hospital, Changsha 410013, Hunan, China.
6. Department of Ultrasonography, Hunan Chest Hospital, Changsha 410013, Hunan, China.

# These authors contributed equally to this work.

✉ Corresponding author: Gaoyan Deng, E-mail: 478376814@qq.com.

Received: 2023.12.01; Accepted: 2024.02.02; Published: 2024.03.04

Abstract

Highly activated aerobic glycolysis provides the metabolic requirements for tumor cell growth and proliferation. Erianin, a natural product isolated from *Dendrobium chrysotoxum Lindl*, has been reported to exert antitumor activity in multiple cancers. However, whether Erianin exerts inhibitory effects on aerobic glycolysis and the inherent mechanism remain poorly defined in non-small cell lung cancer (NSCLC). Here, we showed that Erianin inhibited the cell viability and proliferation, and induced apoptosis in NSCLC cells. Moreover, Erianin overtly suppressed aerobic glycolysis via decreasing HK2 expression. Mechanistically, Erianin dose-dependently curbed the Akt-GSK3β signaling pathway phosphorylation activation, which afterwards downregulated HK2 expression. Meanwhile, Erianin inhibited HCC827 tumor growth *in vivo*. Taken together, our results suggest that the natural product Erianin can suppress aerobic glycolysis and exert potent anticancer effects via the Akt-GSK3β signaling pathway in NSCLC cells.

Keywords: erianin; aerobic glycolysis; HK2; non-small cell lung cancer

Introduction

Lung cancer is the most common cause of cancer-related deaths worldwide, among which non-small cell lung cancer (NSCLC) accounts for 80%-85%[1-4]. Over the past decade, the treatment paradigm for NSCLC has progressed dramatically including chemotherapeutic agents, molecularly targeted drugs, and immune checkpoints inhibitors [5-12]. However, the vast majority of advanced NSCLC become resistant to current treatments and eventually progress[1, 13, 14]. Therefore, the clinical treatment for NSCLC urgently demands identifying novel targets and elucidating underlying mechanisms.

Erianin is a natural product extracted from *Dendrobium chrysotoxum Lindl*[15, 16]. Increasing evidence has manifested that Erianin exerts antitumor properties through diverse molecular mechanisms[16, 17]. Erianin induces apoptosis, blocks angiogenesis, and inhibits cancer progression through the MAPK [18], and mTOR pathways[19, 20]. In lung cancer, Erianin inhibits cell growth and migration via PI3K/Akt pathway[21], and calcium/calmodulin-dependent ferroptosis[22, 23]. Erianin suppresses lung cancer stemness via ferroptosis[24]. These studies imply that Erianin is a potent and promising antitumor agent for clinical treatment.

However, the impact of Erianin on aerobic glycolysis in lung cancer cells remains unclear. In this study, we revealed the inhibitory effects of Erianin on NSCLC cells and found that Erianin significantly

suppressed aerobic glycolysis in NSCLC cells. Herein, we further unveiled the underlying mechanisms of Erianin administration against NSCLC cells.

Materials and methods

Cell culture and antibodies.

Human NSCLC cell HCC827, HCC1975, H1650, and H460 cells were obtained from American Type Culture Collection (ATCC, Manassas, VA). All cells were cultured in DMEM medium supplemented with 10% Fetal Bovine Serum (FBS) and 1% penicillin-streptomycin at 37°C with 5% CO_2. All cells were maintained at the incubator according to the standard protocols and subjected to routinely checking for mycoplasma contamination. Antibodies against HK2 (#2867), Akt (#4691), p-Akt (#4060), cleaved-caspase 3 (#9664), Bax (#14796), VDAC1 (#4661), α-tubulin (#2144), cytochrome c (#4280), Akt1 (#2938), Akt2 (#2964), p-GSK3β (#5558), β-actin (#3700), anti-rabbit IgG HRP (#7074), and anti-mouse IgG HRP (#7076) were obtained from Cell Signaling Technology, Inc. (Beverly, MA). The natural compound Erianin was from Selleck Chemicals (Houston, TX). Necrostatin-1, z-VAD-fmk, and 3-methyladenine were purchased from MedChemExpress (New Jersey, US). Lipofectamine 2000 transfection reagent for transient transfection was purchased from Thermo Fisher Scientific (Waltham, MA).

MTS assay

MTS assay was performed according to the standard protocol[25]. The cultured cells were resuspended and seeded into 96-well plates ($8x10^3$ cells/well) and were incubated at different time points. Cell viability was analyzed with MTS using the Cell Titer 96® Aqueous One Solution kit (Promega Corporation) as determined by the manufacturer's protocol.

Soft Agar Assay

The soft agar assay was performed as described previously[26]. Briefly, the agar base was made with 3 mL of Eagle's basal medium supplemented with 0.6% agar and 10% FBS in a 6-well plate. Cells were collected and counted at $8x10^3$ cells/mL concentration in 1 mL of Eagle's basal medium supplemented with 0.3% agar and 10% FBS overlaid into a 6-well plate with 0.6% agar base. The cells were routinely cultured for 14 days. The colony number was counted with the microscope.

Plate colony formation assay

The cultured cells were exposed to Erianin and were routinely incubated for 2 weeks in a 6-well plate (500 cells/well). When cells formed sufficiently large colonies, cells were fixed with 4% paraformaldehyde for 20 min at 37 ˚C. Cells were stained with 0.5% crystal violet for 5 min at 37 ˚C. The number of colonies was counted with a microscope.

Glycolysis analysis.

The glycolysis analysis was performed as described previously[27]. Glucose consumption and lactate production were analyzed at the Laboratory the Third Xiangya Hospital of Central South University (Changsha, China). The relative glucose consumption and lactate production rate were normalized by protein concentration.

Subcellular Fraction Isolation

The Mitochondria Isolation kit (Thermo Fisher Scientific, Inc.) was used for cytosolic and mitochondrial fraction extraction following the manufacturers' instructions.

Cell Transfection

For transient transfection, the siRNAs, including si-Akt (sc-29195) and siCtrl (sc-37001), were purchased from Santa Cruz Biotechnology (Dallas, TX). The transient transfection was performed using the Lipofectamine 2000 (11668019, Thermo Fisher Scientific) following the manufacturer's protocol. The whole cell extract was prepared at 2 days later after transfection.

Immunoblotting

The immunoblotting (IB) was performed as described previously[28]. Briefly, Cells were lysed in RIPA lysis buffer (Thermo Fisher Scientific, Inc.) containing protease inhibitors to obtain whole-cell extract (WCE), whose concentration was determined by BCA protein assay (Thermo Fisher Scientific, Inc.). Equal amounts of protein (30 μg) were mixed with loading buffer, boiled at 95°C for 5 min, then subjected to SDS-PAGE electrophoresis and transferred onto a PVDF membrane. The membranes were incubated with the primary antibody overnight at 4°C after blocking with 5% non-fat milk at room temperature (RT) for 1 h. Finally, the secondary antibody anti-rabbit/mouse IgG HRP was added and incubated for 30 min at RT, and then the target protein was visualized by chemiluminescence.

Immunofluorescence (IF)

The IF analysis was performed as described previously[29]. Briefly, Cells were fixed in 4% paraformaldehyde (sc-281692; Santa Cruz Biotechnology, Inc.) for 10 min, and permeabilized in 0.2% Triton X-100 (13444259; Thermo Fisher Scientific, Inc.) for 20 min. The slides were incubated with antibodies

overnight at 4°C in a humidified chamber after blocking with 50% goat serum albumin. The next day, the fluorescence-labeled second antibody was added for 40 min at RT. DAPI was used for counterstaining. The stained cell images were obtained using the fluorescence microscope.

Xenograft mouse model

All *in vivo* animal experiments were approved by the Institutional Animal Care and Use Committee (IACUC) of Central South University (Changsha, China). HCC827 cells (2×10^6) in 200 µl DMEM were harvested and subcutaneously inoculated in the right flank of 6-week-old athymic nude mice (n = 6) to generate xenograft models. The tumor volume and body weight of mice were recorded every 2 days. The tumor-bearing mice were randomly divided into two groups when the tumor reached ~100 mm^3. The compound-treated group was administrated Erianin (10 mg/kg every 2 days) by intraperitoneal injection, whereas the control group was administrated the vehicle control. Tumor volume was calculated as length × $width^2$ × 0.5. The mice were euthanized at the endpoint, and the tumor tissues were dissected.

Blood assay

Blood was collected via cardiac puncture of mice with EDTA coating pipes. The red blood cells (RBC), white blood cells (WBC), alanine aminotransferase (ALT), and aspartate aminotransferase (AST) were examined in the laboratory of Central South University of China.

Immunohistochemical staining (IHC)

The IHC staining was performed as described previously[25]. Briefly, the tissues of xenograft tumors were fixed in 10% neutral-buffered formalin. The tissue sections were processed to repair the antigen by the following steps: deparaffinizing, rehydrating, submerging in sodium citrate buffer (10 mM, pH 6.0), and boiling for 10 min. The tissue slides were next treated with 3% H_2O_2 at room temperature for 10 min, washed with PBS, and blocked with 10% goat serum albumin, followed by incubating with primary antibodies overnight at 4 °C and secondary antibodies at room temperature for 45 min. The interested protein was visualized through the DAB substrate incubation and counterstained by hematoxylin. The scores for IHC staining were determined and analyzed by two senior pathologists with a microscope and the Image-Pro Plus software (version 6.2) program (Media Cybernetics). To obtain the scores of the targeted protein we used the calculation formula: percentage scores × intensity scores. The percentage of positive cells was classified into four categories: 0, no positive cells; 1, ≤ 10% positive cells; 2, 10–50% positive cells; 3, > 50% positive cells. The intensity was graded as 0, no staining; 1, weak staining; 2, moderate staining; 3, intense staining. The IHC scores of Ki67, HK2 and p-Akt expression were interpreted as follows: ≤ 2 indicates low expression level; > 2 indicates high expression level.

Statistical analysis

SPSS software (version 13.0; SPSS, Inc.) was used for statistical analysis. The data are presented as the mean ± SD and were analyzed using the Student's t-test or ANOVA. $P<0.05$ was considered to indicate a statistically significant difference.

Results

Erianin inhibits the cell viability and proliferation of NSCLC cells

To determine the inhibitory effect of Erianin on NSCLC cells, we first detected the cell viability of NSCLC cells at indicated time points after exposure to different concentrations of Erianin (Figure 1A). The MTS data indicated that Erianin significantly reduced cell viability in H1975, HCC827, H1650, and H460 cells (Figure 1B and Supplementary Figure 1A). Furthermore, the colony formation ability of NSCLC cells was examined. The results indicated that the colony numbers were dose-dependently reduced with Erianin treatment in H1975, HCC827, H1650, and H460 cells (Figure 1C and Supplementary Figure 1C). Consistently, the immunofluorescence result indicated that higher concentration of Erianin significantly decreased the population of histone H3 Ser10 positive cells (Figure 1D). In contrast, the administration of Erianin had no significant effect on cell viability and colony formation in immortalized non-tumor lung cells NL20 and MRC5 (Supplementary Figure 1B and 1D). Overall, these results suggested that Erianin attenuated the cell viability and proliferation of NSCLC cells.

Erianin suppressed aerobic glycolysis via downregulating HK2 expression in NSCLC cells

Clinically, our analysis results illustrated that high HK2 expression had the worse OS and PFS than low HK2 expression (Supplementary Figure 2A-B). To further determine the effect of Erianin on aerobic glycolysis of NSCLC cells. Exposed to different concentrations of Erianin, the glucose metabolic characteristic was examined among different NSCLC cells. Our data showed that Erianin dose-dependently increased the pH value in H827, HCC1975, and H1650 cells (Figure 2A). Moreover, Erianin significantly dose-dependently decreased the glucose consumption, lactate production, and increased the O_2

consumption ratio in different NSCLC cells, respectively (Figure 2B-E). Hexokinase 2 (HK2), the first-rate limiting enzyme of glucose metabolism, is required for aerobic glycolysis to phosphorylate glucose. Therefore, we further investigated the effect of Erianin on HK2, the IB results showed that Erianin dose-dependently reduced the expression of HK2 protein in HCC827, HCC1975, and H1650 cells (Figure 2F). These results suggested that Erianin suppressed aerobic glycolysis in a HK2-dependent manner in NSCLC cells.

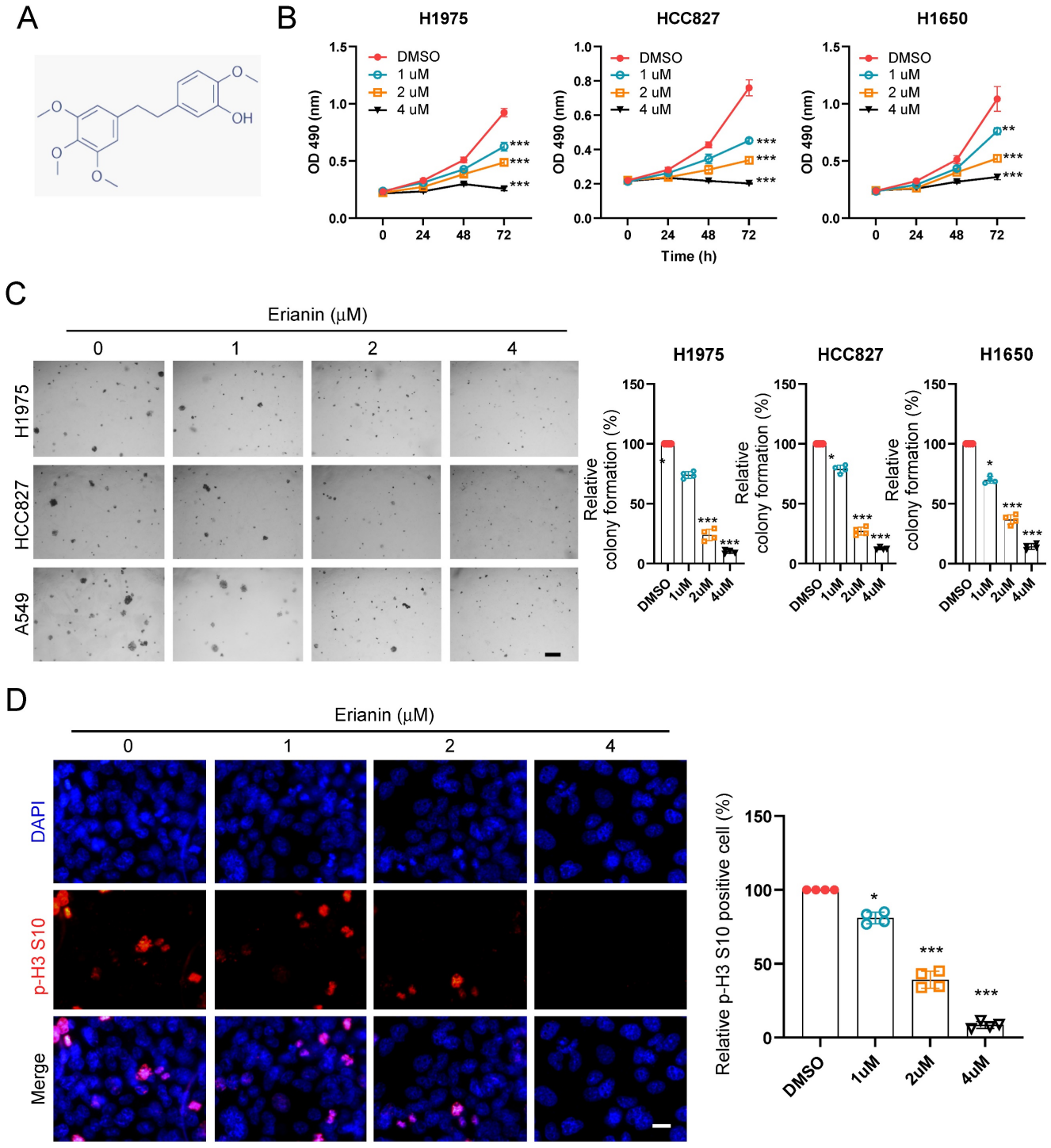

Figure 1. Erianin suppresses cell viability and colony formation of NSCLC cells. (a) Chemical structure of Erianin. (b) H1975, HCC827, and H1650 cells were treated with different concentrations of Erianin (0, 1, 2, 4 μM) for the indicated times. Cell viability was measured using an MTS assay. (c) Colony formation of H1975, HCC827, and H1650 cells were exposed to different concentrations of Erianin (0, 1, 2, 4 μM), Scale bar, 500 μm. (d) HCC827 cells were subjected to Immunofluorescence (IF) analysis with the histone H3 S10 antibody, Scale bar, 10 μm. *, $p < 0.05$, **, $p < 0.01$, ***, $p < 0.001$.

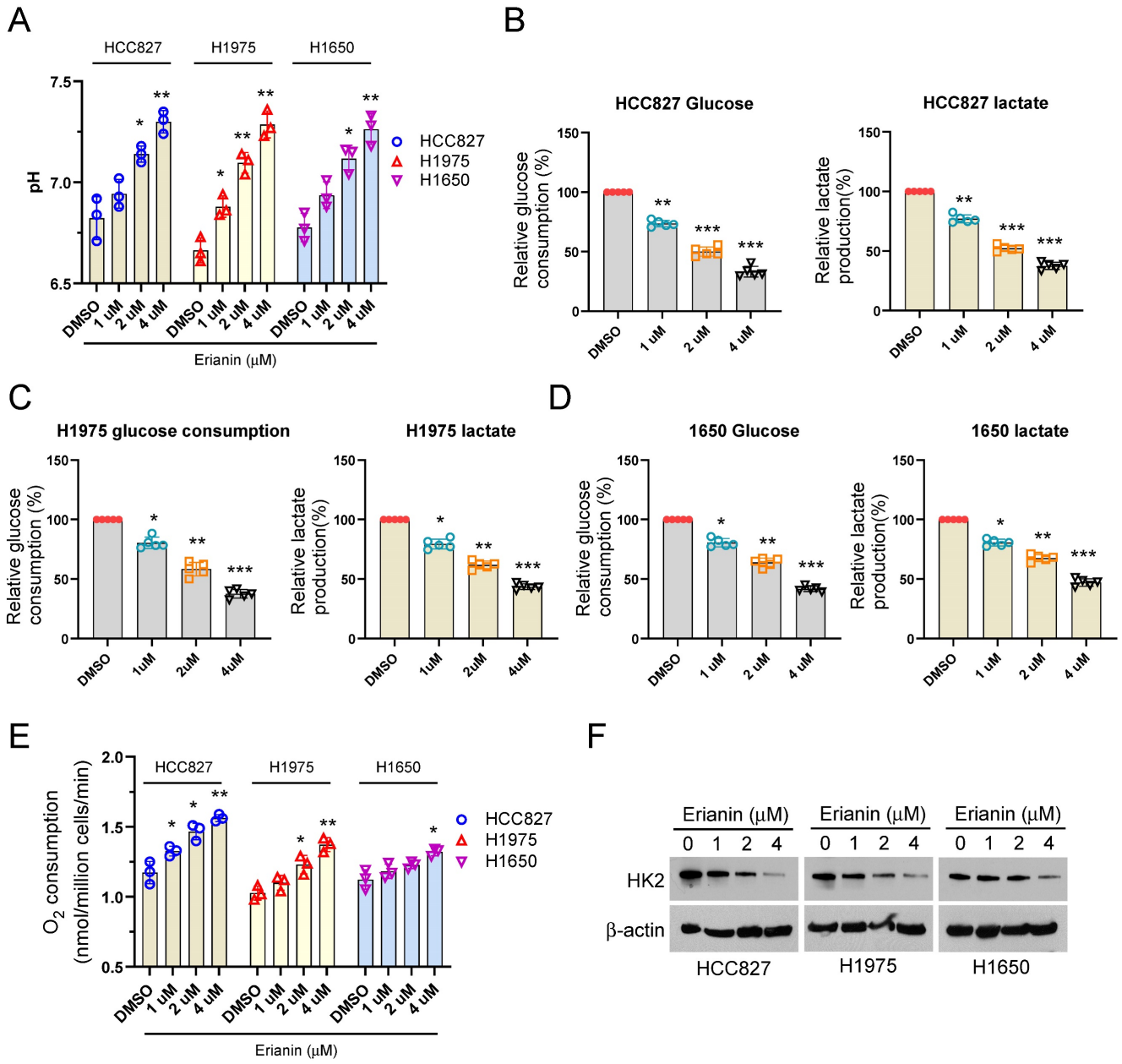

Figure 2. Erianin suppresses HK2 expression and aerobic glycolysis in NSCLC cells. (a-e) Normalized pH value (a), glucose consumption, lactate production, and O_2 consumption (e) in HCC827 (b), H1975 (c), and H1650 (d) cells exposed to different concentrations of Erianin (0, 1, 2, 4 μM), respectively. (f) IB analysis of HK2 in HCC827, H1975, and H1650 cells exposed to different concentrations of Erianin (0, 1, 2, 4 μM). *, $p < 0.05$, **, $p < 0.01$, ***, $p < 0.001$.

Erianin promotes apoptosis to inhibit the cell viability of NSCLC cells

To elucidate the inherent mechanism that Erianin inhibited the cell viability of NSCLC cells. We utilized three cell death inhibitors that inhibited necroptosis, autophagy, and apoptosis, respectively. As shown in Figure 3A, treated with Erianin and the pan-caspase inhibitor z-VAD-fmk, the cell viability was recovered significantly. The results suggested that inhibition of apoptosis rescued Erianin-induced inhibitory effects on NSCLC cells. The IB data showed that Erianin dose-dependently incremented the protein level of cleaved-caspase 3 in HCC827, HCC1975, and H1650 cells (Figure 3B-C). Moreover, the immunofluorescence indicated that Erianin increased the expression of cleaved-caspase 3 in HCC827 cells dose-dependently (Figure 3D). In addition, IB analysis further indicated that Erianin promoted the release of cytochrome c from the mitochondria to the cytoplasm and dose-dependently augmented the expression of Bax in the mitochondrial fraction (Figure 3E), suggesting that Erianin could activate the intrinsic apoptotic pathway. These results indicated that Erianin induced apoptosis in NSCLC cells.

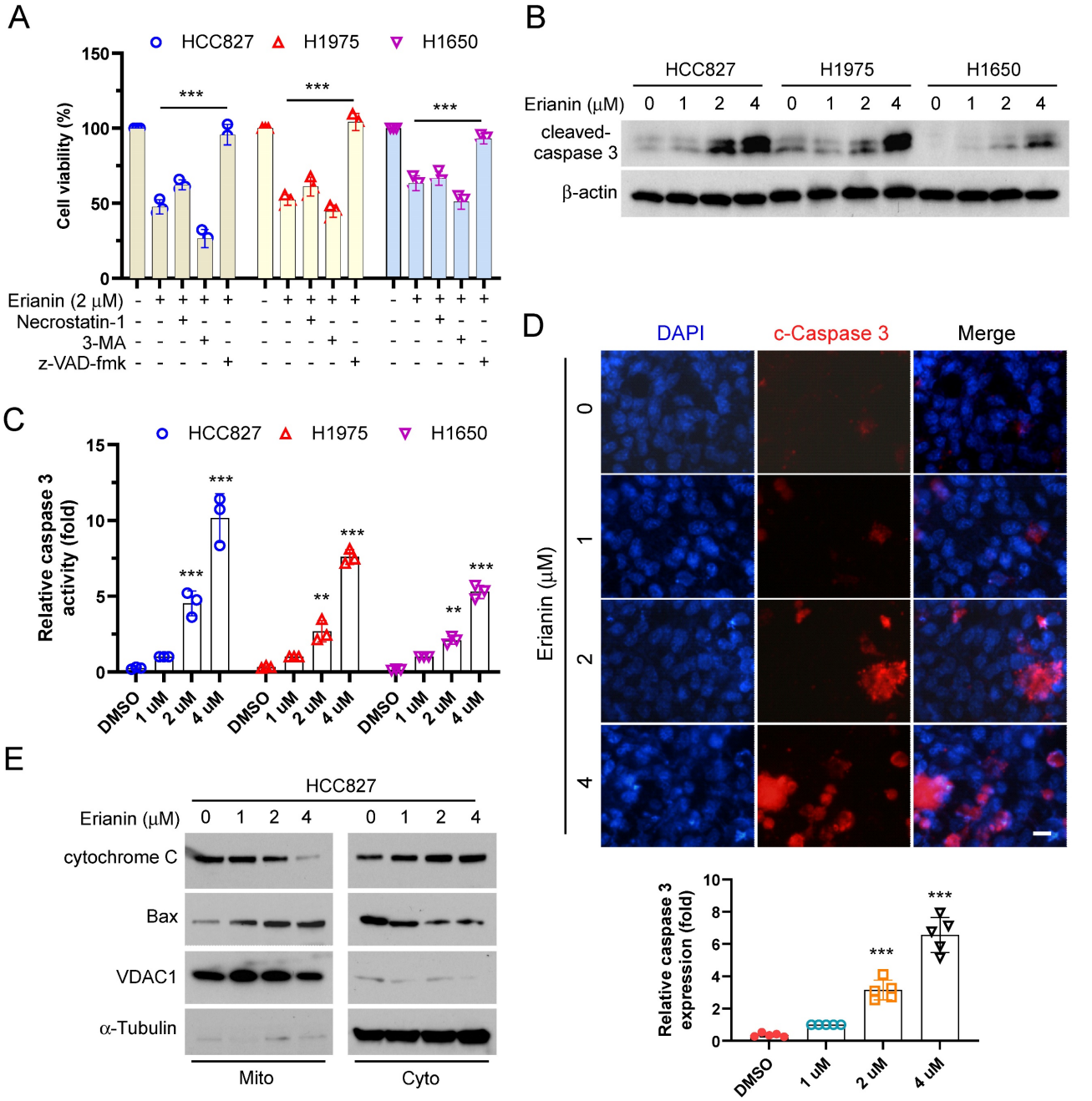

Figure 3. Erianin promotes apoptosis of NSCLC cells. (a) HCC827, H1975, and H1650 cells were treated with 2 μM Erianin combined with Necrostatin-1, z-VAD-fmk, and 3-MA. Cell viability was examined using MTS assay. (b and c) HCC827, H1975, and H1650 cells were treated with different concentrations of Erianin (0, 1, 2, 4 μM) for 24 h. The cell lysate was subjected to IB analysis. (d) HCC827 cells were subjected to Immunofluorescence (IF) analysis with the cleaved-caspase 3 antibody, Scale bar, 10 μm. (e) HCC827 cells were treated with different concentrations of Erianin (0, 1, 2, 4 μM) for 48 h, subcellular fractions were isolated and subjected to IB analysis. *, $p < 0.05$, **, $p < 0.01$, ***, $p < 0.001$. IB, immunoblotting.

Akt is required for Erianin-induced aerobic glycolysis inhibition of NSCLC cells

Our study further determined the inhibitory mechanism of Erianin on aerobic glycolysis in NSCLC cells. We found that Erianin dose-dependently suppressed the phosphorylation of Akt (Figure 4A). Meanwhile, IB analysis indicated that Akt knockdown could decrease the protein level of HK2 (Figure 4B). Likewise, treatment with the kinase inhibitor MK2206, which can specifically reduce the activity of Akt kinase, caused a robust decrease of HK2 protein in HCC827 and HCC1975 cells (Figure 4C). Conversely, in the presence of Erianin, ectopic expression of constitutively activated Akt1 (Myr-Akt1) restored Akt phosphorylation and consistently increased the level of HK2 and the cell viability (Figure 4D-E). The glycolysis analysis results further confirmed that overexpression of Myr-Akt1 enhanced glucose consumption and lactate production (Figure 4F-G).

However, the activity of caspase 3 was obviously inhibited (Figure 4H). Meanwhile, Erianin dose-dependently suppressed the phosphorylation level of GSK3β (Figure 4I-J), which attributed to Erianin-mediated upstream Akt kinase activity inhibition (Figure 4K). Our results illuminated that Erianin inactivated the Akt-GSK3β signaling pathway, and Akt was required for the Erianin-mediated inhibition of aerobic glycolysis on NSCLC cells.

Erianin suppresses tumor growth of NSCLC cells *in vivo*

The xenograft mouse model was constructed to verify the inhibitory effect of Erianin on tumor growth *in vivo*. HCC827-deprived xenograft tumors were exposed to Erianin. The results illustrated that Erianin significantly inhibited the growth of HCC827 tumors compared with the vehicle control (Figure 5A and Figure 5C). The tumor weight of the Erianin-treated group was lower than that of the vehicle-treated group (Figures 5B). Moreover, IHC staining showed that Erianin reduced the expression of phosphorylated Akt and HK2 and decreased the population of Ki-67 positive cells (Figure 5D-E). In addition, the body weight did not change significantly between the Erianin- and vehicle-treated groups (Figure 5F). Erianin treatment did not exhibit specific toxicity on any critical organ functions. When compared to the vehicle-treated group, the levels of red blood cells (RBC), white blood cells (WBC), aspartate transaminase (AST), and alanine transaminase (ALT) were unaffected by Erianin administration (Figure 5G). Overall, these results indicated that the administration of Erianin effectively suppressed tumor growth of NSCLC cells *in vivo*.

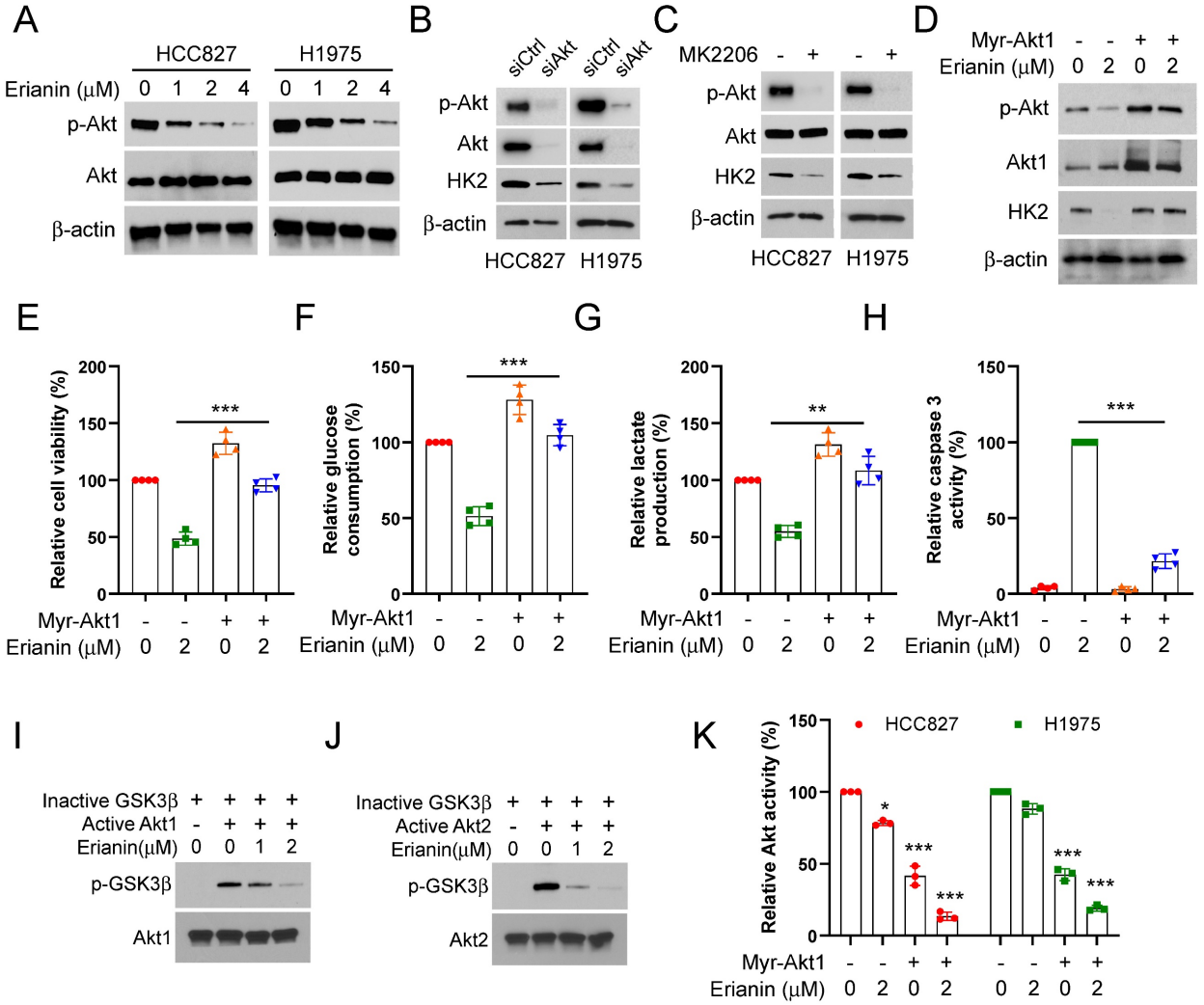

Figure 4. Erianin induces Akt inactivation to inhibit aerobic glycolysis of NSCLC cells. (a) HCC827 and H1975 cells were treated with various concentrations of Erianin, the WCE was subjected to IB assay. (b) HCC827 and H1975 cells were transfected with siCtrl or siAkt for 24h, followed by IB assay. (c) HCC827 and H1975 cells were treated with MK2206 for 24h, followed by IB assay. (d-h) Myr-Akt1 was transfected into HCC827 cells for 24h, followed by 2 μM Erianin treatment. The cell lysate was subjected to IB analysis (d). MTS analysis of cell viability (e). The glucose consumption (f) and lactate production (g) were detected. Caspase 3 activity was determined using the Caspase 3 activity assay (h). (i-j) *In vitro* kinase assay analysis of the inhibitory effect of Erianin on Akt1 (i) and Akt2 (j). (k) Myr-Akt1 was transfected into HCC827 and H1975 cells, followed by Erianin treatment. Akt activity was measured by Akt Kinase Activity Assay Kit. **, $p < 0.01$, ***, $p < 0.001$.

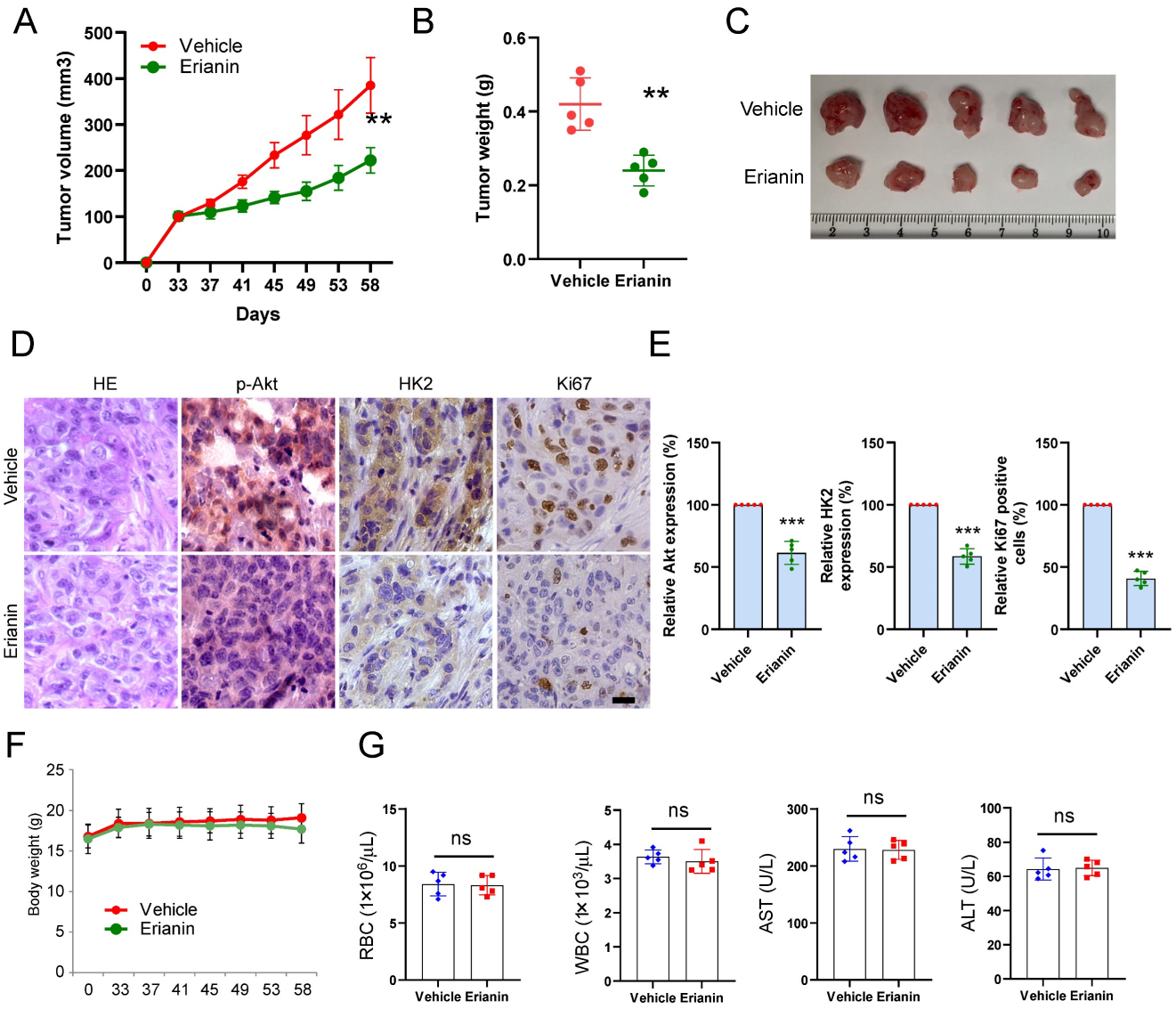

Figure 5. Erianin inhibits *in vivo* tumor growth of NSCLC cells. (a-c) The tumor volume (a), tumor weight (b), and the image of tumor mass (c) of HCC827-derived xenograft tumors treated with vehicle and Erianin. (d-e) The representative images (d) and qualifications (e) of IHC staining of p-Akt, HK2, and Ki67 in HCC827-derived xenograft tumors with Erianin or vehicle treatment. Body weight (f) and mouse blood assay (g) after treatment with erianin or vehicle. Scale bar, 20 μm. **, $p < 0.01$, ***, $p < 0.001$, ns, no significance.

Discussion

Non-small cell lung cancer (NSCLC) is a profoundly devastating disease that is the leading cause of cancer-associated deaths worldwide[30-33]. NSCLC accounts for more than 85% of lung cancer cases, of which lung adenocarcinoma (LUAD) and lung squamous cell carcinoma (LUSC) are the most common subtypes[34-37]. Over the past decade, significant advances have been made in non-small cell lung cancer therapies, Nevertheless, the incidence and mortality have remained increasing, with the predicted 5-year survival rate of 15.9%[38-43]. Aerobic glycolysis, referred to as the Warburg effect, provides the metabolic requirements for tumor cell growth and proliferation[44-47]. It is characterized by increased glucose uptake and lactate production[48-51]. Unlike normal cells that catabolize glucose by oxidative phosphorylation in the mitochondria, tumor cells tend to convert glucose into lactate regardless of oxygen availability[52-55]. Meanwhile, the metabolic intermediates generated during aerobic glycolysis can be used for the biosynthesis of biomacromolecules used by the tumor to meet the demands for rapid growth[56-60]. The lactate production also provides an acidic environment to aid the invasion and metastasis of cancer[61-63]. The first step of glycolysis is catalyzed by hexokinase (HK), which converts glucose to glucose-6-phosphate (G-6-P)[52, 64, 65]. Among four HK isoforms, HK2 is overexpressed in many cancer cells. Han et al.[66] found that the deubiquitinase OTUB1 stabilized MYC and induced

HK2 expression, which leads to the promotion of aerobic glycolysis and breast tumorigenesis. In hepatocellular carcinoma, UBR7 inhibits glycolysis by indirectly suppressing HK2 expression[67]. Thus, we attach much importance to the role of HK2-mediated aerobic glycolysis in NSCLC.

Erianin, a natural product derived from Dendrobium chrysotoxum Lindl[23], has extensive and potent pharmacological activities, including anti-tumor[68], anti-inflammatory[69], and anti-bacterial[20]. Previous studies have demonstrated that Erianin exerted strongly effective anti-tumor effect by promoting apoptosis[21], ferroptosis[70], and autophagy[71], and inhibiting angiogenesis[72]. However, the role of Erianin on aerobic glycolysis in NSCLC remains unclear. In this research, we observed the effect of Erianin on NSCLC cells. Erianin promoted apoptosis and subsequently attenuated the cell viability and proliferation in a dose-dependent manner (Figure 1B-D). Furthermore, our data indicated that Erianin exerted inhibitory effects via suppressing HK2-mediated aerobic glycolysis in NSCLC cells. Erianin significantly dose-dependently decreased glucose consumption and lactate production and reduced the expression of HK2 protein (Figure 2B-F). The results suggested the indispensable role of HK2 in aerobic glycolysis. The inherent mechanism study revealed that Erianin suppressed the phosphorylation of Akt kinase. Akt knockssdown and inhibition could robustly suppress HK2-mediated aerobic glycolysis (Figure 4A-B). However, overexpression of Myr-Akt1 enhanced the glucose consumption and lactate production (Figure 4F-G). Meanwhile, as the downstream target of Akt kinase, Erianin dose-dependently suppressed the phosphorylation level of GSK3β (Figure 4I-K). Therefore, our results illuminated that Erianin inactivated the Akt-GSK3β signaling pathway to inhibit aerobic glycolysis in NSCLC cells.

In summary, our research demonstrated that Erianin was a new aerobic glycolysis inhibitor in NSCLC cells. Our data will hopefully support the use of Erianin as a potential compound for NSCLC treatment *in vitro* and maximize the potential of Erianin for application in the future.

Abbreviations

3-MA: 3-methyladenine; MAPK: mitogen-activated protein kinase; mTOR: mechanistic target of rapamycin; PI3K: phosphoinositide 3-kinase; Akt: protein kinase B; GSK3β: glycogen synthase kinase-3β; HK2: hexokinase 2; IB: immunoblotting; IF: immunofluorescence; OS: overall survival; PFS: progression-free survival.

Supplementary Material

Supplementary figures.
https://www.jcancer.org/v15p2380s1.pdf

Acknowledgements

This work was supported by the Scientific Research Program of Hunan Provincial Health Committee (202203085243).

Competing Interests

The authors have declared that no competing interest exists.

References

1. Wang M, Herbst RS, Boshoff C. Toward personalized treatment approaches for non-small-cell lung cancer. Nat Med. 2021; 27: 1345-56.
2. Miller KD, Nogueira L, Devasia T, Mariotto AB, Yabroff KR, Jemal A, et al. Cancer treatment and survivorship statistics, 2022. CA Cancer J Clin. 2022; 72: 409-36.
3. Yang Y, Liu H, Chen Y, Xiao N, Zheng Z, Liu H, et al. Liquid biopsy on the horizon in immunotherapy of non-small cell lung cancer: current status, challenges, and perspectives. Cell Death Dis. 2023; 14: 230.
4. Zhou H, Guan Q, Hou X, Liu L, Zhou L, Li W, et al. Epithelial-mesenchymal reprogramming by KLF4-regulated Rictor expression contributes to metastasis of non-small cell lung cancer cells. Int J Biol Sci. 2022; 18: 4869-83.
5. Lahiri A, Maji A, Potdar PD, Singh N, Parikh P, Bisht B, et al. Lung cancer immunotherapy: progress, pitfalls, and promises. Mol Cancer. 2023; 22: 40.
6. Yang SR, Schultheis AM, Yu H, Mandelker D, Ladanyi M, Büttner R. Precision medicine in non-small cell lung cancer: Current applications and future directions. Semin Cancer Biol. 2022; 84: 184-98.
7. Leonetti A, Wever B, Mazzaschi G, Assaraf YG, Rolfo C, Quaini F, et al. Molecular basis and rationale for combining immune checkpoint inhibitors with chemotherapy in non-small cell lung cancer. Drug Resist Updat. 2019; 46: 100644.
8. Yang Z, Tam KY. Combination Strategies Using EGFR-TKi in NSCLC Therapy: Learning from the Gap between Pre-Clinical Results and Clinical Outcomes. Int J Biol Sci. 2018; 14: 204-16.
9. Singh S, Yeat NY, Wang YT, Lin SY, Kuo IY, Wu KP, et al. PTPN23 ubiquitination by WDR4 suppresses EGFR and c-MET degradation to define a lung cancer therapeutic target. Cell Death Dis. 2023; 14: 671.
10. Larrue R, Fellah S, Boukrout N, De Sousa C, Lemaire J, Leboeuf C, et al. miR-92a-3p regulates cisplatin-induced cancer cell death. Cell Death Dis. 2023; 14: 603.
11. Stravopodis DJ, Papavassiliou KA, Papavassiliou AG. Vistas in Non-Small Cell Lung Cancer (NSCLC) Treatment: of Kinome and Signaling Networks. Int J Biol Sci. 2023; 19: 2002-5.
12. Lin S, Ruan H, Qin L, Zhao C, Gu M, Wang Z, et al. Acquired resistance to EGFR-TKIs in NSCLC mediates epigenetic downregulation of MUC17 by facilitating NF-κB activity via UHRF1/DNMT1 complex. Int J Biol Sci. 2023; 19: 832-51.
13. Passaro A, Jänne PA, Mok T, Peters S. Overcoming therapy resistance in EGFR-mutant lung cancer. Nat Cancer. 2021; 2: 377-91.
14. Liu Z, Ma L, Sun Y, Yu W, Wang X. Targeting STAT3 signaling overcomes gefitinib resistance in non-small cell lung cancer. Cell Death Dis. 2021; 12: 561.
15. Chen YT, Hsieh MJ, Chen PN, Weng CJ, Yang SF, Lin CW. Erianin Induces Apoptosis and Autophagy in Oral Squamous Cell Carcinoma Cells. Am J Chin Med. 2020; 48: 183-200.
16. Wang H, Zhang T, Sun W, Wang Z, Zuo D, Zhou Z, et al. Erianin induces G2/M-phase arrest, apoptosis, and autophagy via the ROS/JNK signaling pathway in human osteosarcoma cells *in vitro* and *in vivo*. Cell Death Dis. 2016; 7: e2247.
17. Zhang Y, Zhang Q, Wei F, Liu N. Progressive study of effects of erianin on anticancer activity. Onco Targets Ther. 2019; 12: 5457-65.
18. Wang P, Jia X, Lu B, Huang H, Liu J, Liu X, et al. Erianin suppresses constitutive activation of MAPK signaling pathway by inhibition of CRAF and MEK1/2. Signal Transduct Target Ther. 2023; 8: 96.
19. Mo C, Shetti D, Wei K. Erianin Inhibits Proliferation and Induces Apoptosis of HaCaT Cells via ROS-Mediated JNK/c-Jun and AKT/mTOR Signaling Pathways. Molecules. 2019; 24(15): 2727.

20. Yang Z, Liu R, Qiu M, Mei H, Hao J, Song T, et al. The roles of ERIANIN in tumor and innate immunity and its' perspectives in immunotherapy. Front Immunol. 2023; 14: 1170754.
21. Zhang HQ, Xie XF, Li GM, Chen JR, Li MT, Xu X, et al. Erianin inhibits human lung cancer cell growth via PI3K/Akt/mTOR pathway *in vitro* and *in vivo*. Phytother Res. 2021; 35: 4511-25.
22. Chen P, Wu Q, Feng J, Yan L, Sun Y, Liu S, et al. Erianin, a novel dibenzyl compound in Dendrobium extract, inhibits lung cancer cell growth and migration via calcium/calmodulin-dependent ferroptosis. Signal Transduct Target Ther. 2020; 5: 51.
23. Li G, Zhang H, Lai H, Liang G, Huang J, Zhao F, et al. Erianin: A phytoestrogen with therapeutic potential. Front Pharmacol. 2023; 14: 1197056.
24. Lv J, Wang Z, Liu H. Erianin suppressed lung cancer stemness and chemotherapeutic sensitivity via triggering ferroptosis. Environ Toxicol. 2024; 39: 479-86.
25. Han S, Yu X, Wang R, Wang X, Liu L, Zhao Q, et al. Tanshinone IIA inhibits cell viability and promotes PUMA-mediated apoptosis of oral squamous cell carcinoma. J Cancer. 2023; 14: 2481-90.
26. Li M, Liu H, Zhao Q, Han S, Zhou L, Liu W, et al. Targeting Aurora B kinase with Tanshinone IIA suppresses tumor growth and overcomes radioresistance. Cell Death Dis. 2021; 12: 152.
27. Li W, Gao F, Ma X, Wang R, Dong X, Wang W. Deguelin inhibits non-small cell lung cancer via down-regulating Hexokinases II-mediated glycolysis. Oncotarget. 2017; 8: 32586-99.
28. Li X, Liang Q, Zhou L, Deng G, Xiao Y, Gan Y, et al. Survivin degradation by bergenin overcomes pemetrexed resistance. Cell Oncol (Dordr). 2023; 46: 1837-53.
29. Liu W, Li W, Liu H, Yu X. Xanthohumol inhibits colorectal cancer cells via downregulation of Hexokinases II-mediated glycolysis. Int J Biol Sci. 2019; 15: 2497-508.
30. Sung H, Ferlay J, Siegel RL, Laversanne M, Soerjomataram I, Jemal A, et al. Global Cancer Statistics 2020: GLOBOCAN Estimates of Incidence and Mortality Worldwide for 36 Cancers in 185 Countries. CA Cancer J Clin. 2021; 71: 209-49.
31. Yang H, Zhao J, Zhao M, Zhao L, Zhou LN, Duan Y, et al. GDC-0349 inhibits non-small cell lung cancer cell growth. Cell Death Dis. 2020; 11: 951.
32. Zhao J, Wang X, Mi Z, Jiang X, Sun L, Zheng B, et al. STAT3/miR-135b/NF-κB axis confers aggressiveness and unfavorable prognosis in non-small-cell lung cancer. Cell Death Dis. 2021; 12: 493.
33. Zhao Y, Guo S, Deng J, Shen J, Du F, Wu X, et al. VEGF/VEGFR-Targeted Therapy and Immunotherapy in Non-small Cell Lung Cancer: Targeting the Tumor Microenvironment. Int J Biol Sci. 2022; 18: 3845-58.
34. Relli V, Trerotola M, Guerra E, Alberti S. Abandoning the Notion of Non-Small Cell Lung Cancer. Trends Mol Med. 2019; 25: 585-94.
35. Srivastava S, Mohanty A, Nam A, Singhal S, Salgia R. Chemokines and NSCLC: Emerging role in prognosis, heterogeneity, and therapeutics. Semin Cancer Biol. 2022; 86: 233-46.
36. Liang J, Li H, Han J, Jiang J, Wang J, Li Y, et al. Mex3a interacts with LAMA2 to promote lung adenocarcinoma metastasis via PI3K/AKT pathway. Cell Death Dis. 2020; 11: 614.
37. Yu T, Nie FQ, Zhang Q, Yu SK, Zhang ML, Wang Q, et al. Effects of methionine deficiency on B7H3-DAP12-CAR-T cells in the treatment of lung squamous cell carcinoma. Cell Death Dis. 2024; 15: 12.
38. Chen Z, Fillmore CM, Hammerman PS, Kim CF, Wong KK. Non-small-cell lung cancers: a heterogeneous set of diseases. Nat Rev Cancer. 2014; 14: 535-46.
39. Ettinger DS, Akerley W, Borghaei H, Chang AC, Cheney RT, Chirieac LR, et al. Non-small cell lung cancer, version 2.2013. J Natl Compr Canc Netw. 2013; 11: 645-53; quiz 53.
40. Socinski MA, Obasaju C, Gandara D, Hirsch FR, Bonomi P, Bunn P, et al. Clinicopathologic Features of Advanced Squamous NSCLC. J Thorac Oncol. 2016; 11: 1411-22.
41. Liu X, Wang X, Chai B, Wu Z, Gu Z, Zou H, et al. miR-199a-3p/5p regulate tumorgenesis via targeting Rheb in non-small cell lung cancer. Int J Biol Sci. 2022; 18: 4187-202.
42. Tang Z, Du W, Xu F, Sun X, Chen W, Cui J, et al. Icariside II enhances cisplatin-induced apoptosis by promoting endoplasmic reticulum stress signalling in non-small cell lung cancer cells. Int J Biol Sci. 2022; 18: 2060-74.
43. Luo Y, Ma S, Sun Y, Peng S, Zeng Z, Han L, et al. MUC3A induces PD-L1 and reduces tyrosine kinase inhibitors effects in EGFR-mutant non-small cell lung cancer. Int J Biol Sci. 2021; 17: 1671-81.
44. Vander Heiden MG, Cantley LC, Thompson CB. Understanding the Warburg effect: the metabolic requirements of cell proliferation. Science. 2009; 324: 1029-33.
45. Guo D, Tong Y, Jiang X, Meng Y, Jiang H, Du L, et al. Aerobic glycolysis promotes tumor immune evasion by hexokinase2-mediated phosphorylation of IκBα. Cell Metab. 2022; 34: 1312-24.e6.
46. Li M, Gao F, Zhao Q, Zuo H, Liu W, Li W. Tanshinone IIA inhibits oral squamous cell carcinoma via reducing Akt-c-Myc signaling-mediated aerobic glycolysis. Cell Death Dis. 2020; 11: 381.
47. Li S, Gao J, Zhuang X, Zhao C, Hou X, Xing X, et al. Cyclin G2 Inhibits the Warburg Effect and Tumour Progression by Suppressing LDHA Phosphorylation in Glioma. Int J Biol Sci. 2019; 15: 544-55.
48. Song H, Li D, Wang X, Fang E, Yang F, Hu A, et al. HNF4A-AS1/hnRNPU/CTCF axis as a therapeutic target for aerobic glycolysis and neuroblastoma progression. J Hematol Oncol. 2020; 13: 24.
49. Kocianova E, Piatrikova V, Golias T. Revisiting the Warburg Effect with Focus on Lactate. Cancers (Basel). 2022; 14(24): 6028.
50. Hsieh YT, Tu HF, Yang MH, Chen YF, Lan XY, Huang CL, et al. Mitochondrial genome and its regulator TFAM modulates head and neck tumourigenesis through intracellular metabolic reprogramming and activation of oncogenic effectors. Cell Death Dis. 2021; 12: 961.
51. Guan Y, Yao W, Yu H, Feng Y, Zhao Y, Zhan X, et al. Chronic stress promotes colorectal cancer progression by enhancing glycolysis through β2-AR/CREB1 signal pathway. Int J Biol Sci. 2023; 19: 2006-19.
52. Feng J, Li J, Wu L, Yu Q, Ji J, Wu J, et al. Emerging roles and the regulation of aerobic glycolysis in hepatocellular carcinoma. J Exp Clin Cancer Res. 2020; 39: 126.
53. Kato Y, Maeda T, Suzuki A, Baba Y. Cancer metabolism: New insights into classic characteristics. Jpn Dent Sci Rev. 2018; 54: 8-21.
54. Jiang H, Wei H, Wang H, Wang Z, Li J, Ou Y, et al. Zeb1-induced metabolic reprogramming of glycolysis is essential for macrophage polarization in breast cancer. Cell Death Dis. 2022; 13: 206.
55. Dong F, Li H, Liu L, Yao LL, Wang J, Xiang D, et al. ACE2 negatively regulates the Warburg effect and suppresses hepatocellular carcinoma progression via reducing ROS-HIF1α activity. Int J Biol Sci. 2023; 19: 2613-29.
56. Lunt SY, Vander Heiden MG. Aerobic glycolysis: meeting the metabolic requirements of cell proliferation. Annu Rev Cell Dev Biol. 2011; 27: 441-64.
57. Hui S, Ghergurovich JM, Morscher RJ, Jang C, Teng X, Lu W, et al. Glucose feeds the TCA cycle via circulating lactate. Nature. 2017; 551: 115-8.
58. Li J, Zhang Q, Guan Y, Liao D, Jiang D, Xiong H, et al. Circular RNA circVAMP3 promotes aerobic glycolysis and proliferation by regulating LDHA in renal cell carcinoma. Cell Death Dis. 2022; 13: 443.
59. Zheng Y, Zhan Y, Zhang Y, Zhang Y, Liu Y, Xie Y, et al. Hexokinase 2 confers radio-resistance in hepatocellular carcinoma by promoting autophagy-dependent degradation of AIMP2. Cell Death Dis. 2023; 14: 488.
60. Tantai J, Pan X, Chen Y, Shen Y, Ji C. TRIM46 activates AKT/HK2 signaling by modifying PHLPP2 ubiquitylation to promote glycolysis and chemoresistance of lung cancer cells. Cell Death Dis. 2022; 13: 285.
61. Lin J, Liu G, Chen L, Kwok HF, Lin Y. Targeting lactate-related cell cycle activities for cancer therapy. Semin Cancer Biol. 2022; 86: 1231-43.
62. Paul S, Ghosh S, Kumar S. Tumor glycolysis, an essential sweet tooth of tumor cells. Semin Cancer Biol. 2022; 86: 1216-30.
63. Kornberg MD, Bhargava P, Kim PM, Putluri V, Snowman AM, Putluri N, et al. Dimethyl fumarate targets GAPDH and aerobic glycolysis to modulate immunity. Science. 2018; 360: 449-53.
64. Lis P, Dyląg M, Niedźwiecka K, Ko YH, Pedersen PL, Goffeau A, et al. The HK2 Dependent "Warburg Effect" and Mitochondrial Oxidative Phosphorylation in Cancer: Targets for Effective Therapy with 3-Bromopyruvate. Molecules. 2016; 21(12): 1730.
65. Seiler K, Humbert M, Minder P, Mashimo I, Schläfli AM, Krauer D, et al. Hexokinase 3 enhances myeloid cell survival via non-glycolytic functions. Cell Death Dis. 2022; 13: 448.
66. Han X, Ren C, Lu C, Qiao P, Yang T, Yu Z. Deubiquitination of MYC by OTUB1 contributes to HK2 mediated glycolysis and breast tumorigenesis. Cell Death Differ. 2022; 29: 1864-73.
67. Zhao L, Kang M, Liu X, Wang Z, Wang Y, Chen H, et al. UBR7 inhibits HCC tumorigenesis by targeting Keap1/Nrf2/Bach1/HK2 and glycolysis. J Exp Clin Cancer Res. 2022; 41: 330.
68. Ma L, Li M, Zhang Y, Liu K. Recent advances of antitumor leading compound Erianin: Mechanisms of action and structural modification. Eur J Med Chem. 2023; 261: 115844.
69. Zhang X, Hu L, Xu S, Ye C, Chen A. Erianin: A Direct NLRP3 Inhibitor With Remarkable Anti-Inflammatory Activity. Front Immunol. 2021; 12: 739953.
70. Xiang Y, Chen X, Wang W, Zhai L, Sun X, Feng J, et al. Natural Product Erianin Inhibits Bladder Cancer Cell Growth by Inducing Ferroptosis via NRF2 Inactivation. Front Pharmacol. 2021; 12: 775506.

71. Miao Q, Deng WQ, Lyu WY, Sun ZT, Fan SR, Qi M, et al. Erianin inhibits the growth and metastasis through autophagy-dependent ferroptosis in KRAS(G13D) colorectal cancer. Free Radic Biol Med. 2023; 204: 301-12.
72. Li X, Liu X, Xing Y, Zeng L, Liu X, Shen H, et al. Erianin Controls Collagen-Mediated Retinal Angiogenesis via the RhoA/ROCK1 Signaling Pathway Induced by the alpha2/beta1 Integrin-Collagen Interaction. Invest Ophthalmol Vis Sci. 2022; 63: 27.